

# ADAPTIVE FREQUENCY DOMAIN ALIGNMENT NETWORK FOR MEDICAL IMAGE SEGMENTATION

Zhanwei Li, Liang Li\* and Jiawan Zhang

College of Intelligence and Computing, Tianjin University  
Tianjin 300350, PR China

## ABSTRACT

High-quality annotated data plays a crucial role in achieving accurate segmentation. However, such data for medical image segmentation are often scarce due to the time-consuming and labor-intensive nature of manual annotation. To address this challenge, we propose the *Adaptive Frequency Domain Alignment Network (AFDAN)*—a novel domain adaptation framework designed to align features in the frequency domain and alleviate data scarcity. AFDAN integrates three core components to enable robust cross-domain knowledge transfer: an *Adversarial Domain Learning Module* that transfers features from the source to the target domain; a *Source-Target Frequency Fusion Module* that blends frequency representations across domains; and a *Spatial-Frequency Integration Module* that combines both frequency and spatial features to further enhance segmentation accuracy across domains. Extensive experiments demonstrate the effectiveness of AFDAN: it achieves an Intersection over Union (IoU) of 90.9% for vitiligo segmentation in the newly constructed VITILIGO2025 dataset and a competitive IoU of 82.6% on the retinal vessel segmentation benchmark DRIVE, surpassing existing state-of-the-art approaches.

**Index Terms**—domain adaptation, frequency alignment, adversarial learning, medical image segmentation

## 1. INTRODUCTION

For large-scale medical image segmentation, high-quality annotated data are essential for achieving accurate model performance. However, due to the heavy reliance on expert domain knowledge and the substantial costs of annotation, such data remain scarce in most practical scenarios. This scarcity severely constrains model generalization, particularly in target domains characterized by complex data distributions or limited sample availability [1].

To address these limitations, transferring knowledge from existing annotated datasets in related domains has emerged as a valuable research direction[2]. However, most current approaches operate under the assumption that the source and

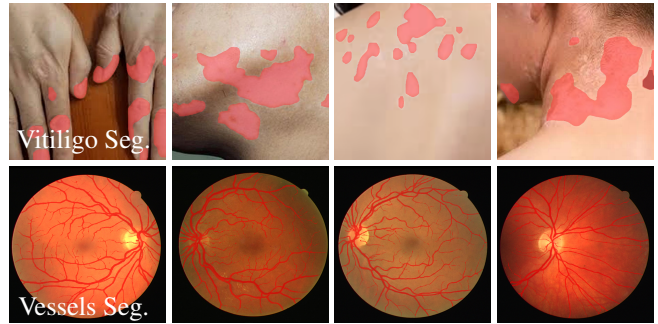


**Fig. 1.** Segmentation results for vitiligo (first row) and retinal vessels (second row). Predicted regions are highlighted in red (best viewed in color). Note that both results were obtained without direct training on datasets annotated specifically for these target structures: the vitiligo segmentation model was trained using skin lesion annotations, while the retinal vessel segmentation was derived from a model trained with general fundus image annotations.

target domains share identical or highly similar annotation categories. For instance, Jeon *et al.* [3] directly apply models pre-trained on public datasets to multi-organ segmentation tasks. In real-world clinical settings, such assumptions rarely hold. To illustrate, the source domain may contain only annotations of normal anatomical structures, whereas the target task requires the segmentation of pathological regions, or the source may include multi-class annotations while the target focuses on only a subset. The *annotation discrepancy* significantly complicates knowledge transfer across domains, frequently leading to negative transfer or the failure of domain adaptation.

Recent studies [4, 5] have sought to mitigate inter-domain distribution gaps through methods such as partial feature alignment[6], pseudo-label generation[7], and label mapping[8]. Nonetheless, most of these approaches do not adequately resolve the deeper semantic gap introduced by mismatched annotation spaces [9]. Developing transfer learning frameworks that account for annotation disparities to enable effective knowledge transfer and semantic structural alignment remains a critical yet underexplored challenge.

\*Corresponding author: ✉ liangli@tju.edu.cn

By decoupling structural (phase) and semantic (amplitude) information, the frequency-domain approach minimizes its impact on the semantic content of images[10]. This inherent property makes it less susceptible to negative transfer and more focused on capturing domain-invariant representations. In this work, we address the challenge of annotation discrepancies in medical image segmentation by introducing the *Adaptive Frequency Domain Alignment Network (AFDAN)*. Our contributions are as follows.

1. We propose AFDAN, a novel cross-domain segmentation network. It integrates three key modules: the Adversarial Domain Learning (ADL) module, the Source-Target Frequency Fusion (STFF) module, and the Spatial-Frequency Integration (SFI) module. Specifically, the ADL module generates target-specific frequency features from source domain images to enable effective cross-domain alignment; the STFF module accelerates the construction of target domain frequency features, thereby improving both efficiency and adaptability; and the SFI module combines complementary representations from the frequency and spatial domains to further enhance segmentation accuracy and preserve fine anatomical structures. Collectively, these components reduce domain shift, preserve structural detail, and improve the detection of subtle lesions.
2. We conduct comprehensive experiments across multiple benchmarks. AFDAN achieves state-of-the-art performance, with an Intersection over Union (IoU) of 90.9% on the newly constructed VITILIGO2025 dataset [11] and 82.6% on the DRIVE [12] retinal vessel segmentation benchmark. As illustrated in Fig. 1, the segmentation outputs exhibit high visual fidelity, accurately delineating structural details across both normal and pathological regions.

## 2. METHOD

This section introduces three core modules of the proposed model AFDAN. The overall architecture of AFDAN and the relationship between three modules is shown in Fig. 2.

### 2.1. Adversarial Domain Learning Module

Inspired by DANN [2], we employ an Adversarial Domain Learning module to align features from source and target domains, as shown in Fig. 2. Given the observation that amplitude spectrum contains domain-specific style characteristics [13], we propose a frequency-aware adversarial learning strategy specifically designed for amplitude spectrum alignment. Denoting the discriminator and generator as  $D$  and  $G$  respectively, the adversarial loss is defined as:

$$\mathcal{L}_{AD} = \mathbb{E}_{A_t} [\log D(A_t)] + \mathbb{E}_{A_s} [\log (1 - D(G(A_s)))] , (1)$$

where  $A_s$  and  $A_t$  denote the amplitude spectra of the source and target domains, respectively. Optimizing this adversarial objective encourages the generator  $G$  to produce amplitude representations  $G(A_s)$  that are indistinguishable from  $A_t$  to the discriminator  $D$ , thereby effectively aligning the source amplitude distribution with the target domain. Notably, our Adversarial Domain Learning module plays an indispensable role in alleviating annotation discrepancies between the source and target domains.

### 2.2. Source-Target Frequency Fusion Module

Motivated by the need to accelerate domain adaptation and prevent overfitting, we introduce a Source-Target Frequency Fusion module. Fourier analysis indicates that the phase spectrum primarily encodes structural information, while the amplitude spectrum governs intensity distribution—a finding leveraged in domain adaptation to improve structural consistency across domains [14]. Our module preserves the source phase to retain critical structures (e.g., lesion contours) and aligns only the amplitude across domains, thereby maintaining anatomical integrity while adapting appearance [15].

For source-domain features  $F_s \in \mathbb{R}^{B \times C \times H \times W}$  from  $x_s$  and target-domain features  $F_t \in \mathbb{R}^{B \times C \times H \times W}$  from  $x_t$ , where  $x_s$  denotes source-domain images and  $x_t$  denotes target-domain images, we decompose them via 2D FFT as:

$$F_s = A_s e^{i\Phi_s}, \quad F_t = A_t e^{i\Phi_t}, \quad (2)$$

where  $A_s, A_t$  represent amplitude spectra from both domains and  $\Phi_s, \Phi_t \in [-\pi, \pi]^{B \times C \times H \times W}$  denote phase spectra.

To align intensity distributions without compromising anatomical integrity, we directly retain the source domain’s phase spectrum to preserve structural consistency. For amplitude alignment while retaining their respective high-frequency components to maintain important structural details [16], we fuse the low-frequency components of the source and target amplitude spectra via:

$$A_{\text{fusion, LF}} = \alpha \cdot A_s + (1 - \alpha) \cdot A_t, \quad (3)$$

where  $\alpha \sim \mathcal{U}(0, 1)$  is a random mixing coefficient drawn from a uniform distribution. This stochastic fusion strategy constructs dense intermediate amplitude distributions between domains, thereby effectively facilitating the reduction of annotation discrepancies.

### 2.3. Spatial-Frequency Integration Module

Our efficient architecture integrates spatial-frequency features, which is critical for capturing both global context and local edge details [17]. To handle spatial dimension mismatches between frequency features ( $F_{\text{freq}}^k$ , where  $k = 1, 2, 3, 4$ , corresponding to features with distinct output dimensions) and spatial features ( $F_{\text{spa}}^k$ ), we use bilinear interpolation to resample  $F_{\text{freq}}^k$  to match the size of  $F_{\text{spa}}^k$  while

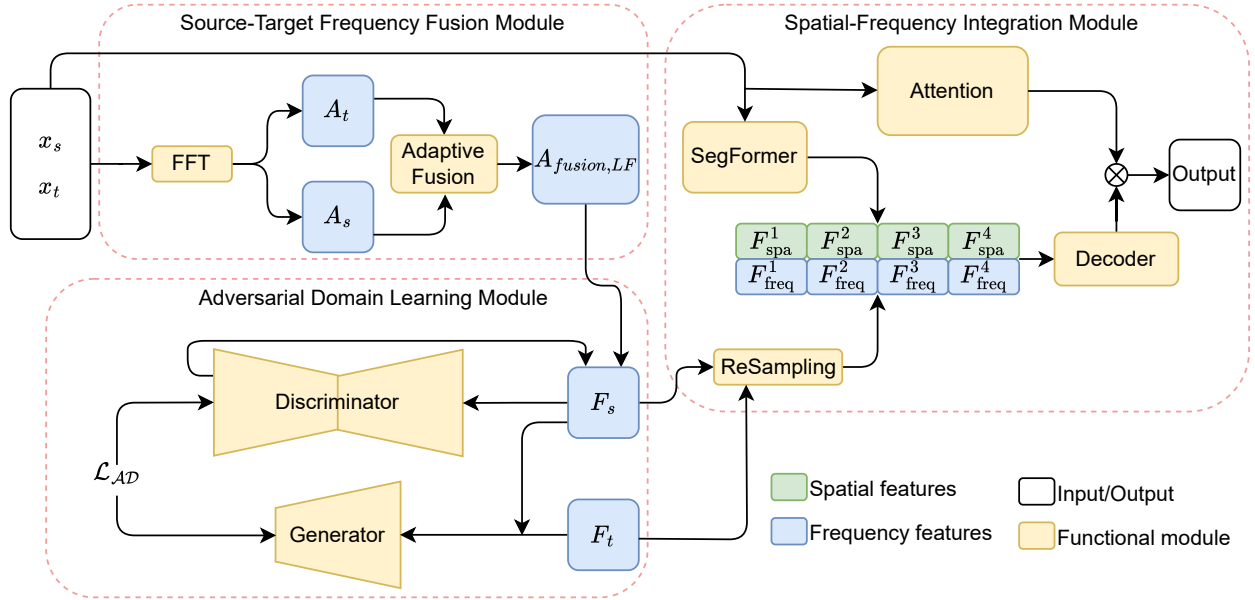


**Fig. 2.** The source and target domain images,  $x_s$  and  $x_t$ , are first transformed into the frequency domain via Fast Fourier transform (FFT). An Adaptive Fusion mechanism is then applied to accelerate domain adaptation. The second module, the Adversarial Domain Learning module, reduces domain shift, where  $F_t$  denotes the target-domain features. Finally, the spatial and frequency features are jointly fed into the Spatial-Frequency Integration module. The integrated features are then concatenated, passed through the decoder, and multiplied with the attention map to produce the segmentation result, enabling effective integration of spatial and frequency features.

preserving spatial relationships. The aligned features are then concatenated channel-wise into  $F_{cat}^k$ , effectively combining complementary frequency-based structural cues and spatial semantic information.

An attention mechanism is further introduced to suppress specialized noise (e.g., device artifacts) and highlight domain-invariant regions [18]. The concatenated features are processed by a decoder to recover structural and contextual details, after which the output is modulated via element-wise multiplication with a spatial attention map to produce the final segmentation. This design enhances discriminative power and emphasizes task-relevant patterns, improving overall robustness and accuracy. As illustrated in Fig. 2, our framework leverages the modular and replaceable design of SegFormer [19], allowing flexible component selection based on task complexity and dataset scale.

### 3. EXPERIMENT

#### 3.1. Dataset

To tackle annotation scarcity in medical image segmentation, we propose a cross-domain training approach evaluated through two complementary experiments.

For the vitiligo segmentation task, we first adopt a cross-

domain setup: the ISIC2018 dataset [20] serves as the source domain, providing dermatoscopic images with high-quality masks across multiple skin diseases to enable robust feature learning. The target domain consists of expert-annotated VITILIGO2025 dataset [11], which focuses on vitiligo and offers precise segmentation masks validated by dermatologists.

**Table 1.** Performance on Vitiligo and Retinal Vessel Segmentation Tasks

Dataset	Model	IoU (%)
<i>(a) Vitiligo Segmentation</i>		
VITILIGO2025	SegFormer	76.8
VITILIGO2025 + ISIC2018	SegFormer	80.3
VITILIGO2025 + ISIC2018	AFDAN	90.9
<i>(b) Retinal Vessel Segmentation</i>		
DRIVE	SegFormer	78.1
DRIVE + Fundus-AVSeg	SegFormer	76.5
DRIVE + Fundus-AVSeg	AFDAN	82.6

The second set of experiments evaluates performance on retinal vessel segmentation. We use the Fundus-AVSeg dataset [28] as the source domain, which provides high-resolution fundus images with pixel-level artery/vein annotations and quality assessment metrics. The target domain is the DRIVE dataset [12], a widely recognized benchmark

**Table 2.** Performance comparison (in %) of different segmentation models on VITILIGO2025 and DRIVE datasets.

Type	Model	VITILIGO2025		DRIVE	
		IoU	Dice	IoU	Dice
Traditional Model	PSPNet [21]	78.0	87.5	68.5	81.3
	SAM2 [22]	84.5	91.6	74.5	85.4
	SimCIS [23]	85.8	92.4	75.2	85.8
	CMFormer [24]	87.2	93.2	76.1	86.4
	YOLO11 [25]	88.5	93.9	77.8	87.5
Domain Adaptation	EHTDI[26]	89.2	94.3	79.5	88.6
	DSTC-SSDA[27]	89.8	94.6	80.2	89.0
	<b>AFDAN (Ours)</b>	<b>90.9</b>	<b>95.2</b>	<b>82.6</b>	<b>90.5</b>

containing fundus images and manually segmented vessel maps, with dual-expert annotations in the test set ensuring fair evaluation of model generalization.

As shown in Table 1, the incorporation of source domain data plays an indispensable role in enabling effective cross-domain knowledge transfer. On both vitiligo and retinal vessel segmentation tasks, our AFDAN model consistently demonstrates the ability to transfer prior knowledge from source to target domains, thereby significantly compensating for the limited annotations in specialized medical image segmentation tasks.

### 3.2. Comprehensive Metric-Based Evaluation of Segmentation Models

We evaluated 8 segmentation models on two medical datasets using core metrics (IoU, Dice; Table 2). Among traditional models, performance showed a consistent upward trend across both datasets: PSPNet [21] achieved the lowest IoU (78.0% on VITILIGO2025, 68.5% on DRIVE), while YOLO11 [25] emerged as the top traditional model (88.5% IoU/93.9% Dice on VITILIGO2025; 77.8% IoU/87.5% Dice on DRIVE). Domain adaptation models outperformed traditional ones on both datasets: EHTDI [26] and DSTC-SSDA [27] reached 89.2%–89.8% IoU on VITILIGO2025 and 79.5%–80.2% IoU on DRIVE. Our AFDAN achieved the best performance across all metrics and datasets: 90.9% IoU/95.2% Dice on VITILIGO2025 (+2.4% IoU vs. YOLO11) and 82.6% IoU/90.5% Dice on DRIVE (+4.8% IoU vs. YOLO11). These results validate the effectiveness of our proposed method for medical image segmentation.

### 3.3. Ablation Studies

To validate the effectiveness and generalizability of each core component in AFDAN, we conduct ablation studies on both the VITILIGO2025 and DRIVE datasets. Table 3 summarizes the IoU (%) results across both tasks, demonstrating consistent contributions of each module.

**Table 3.** Module effectiveness verification results on vitiligo (VITILIGO2025) and retinal vessel (DRIVE) segmentation.

Configuration	IoU (%)	
	Vitiligo	Retinal Vessel
Baseline	80.3	76.5
+ STFF	84.4 (+4.1)	78.6 (+2.1)
+ ADL	83.9 (+3.6)	77.4 (+0.9)
+ SFI	85.2 (+4.9)	78.2 (+1.7)
+ STFF + ADL	86.3 (+6.0)	79.2 (+2.7)
+ STFF + SFI	88.1 (+7.8)	81.3 (+4.8)
<b>Full Model</b>	<b>90.9 (+10.6)</b>	<b>82.6 (+6.1)</b>

To validate AFDAN’s core components’ effectiveness and generalizability, we perform ablation studies on VITILIGO2025 (vitiligo) and DRIVE (retinal vessel) datasets, assessing each module’s performance contribution. Table 3 shows the **Baseline** (SegFormer without AFDAN’s modules) achieves 80.3% IoU (vitiligo) and 76.5% IoU (retinal vessel) as references. Each module boosts performance on both tasks: **STFF** (frequency alignment for style discrepancy reduction) delivers the largest single-module gains (+4.1% vitiligo, +2.1% DRIVE); **ADL** improves feature invariance to domain shift (+3.6% vitiligo, +0.9% DRIVE); **SFI** (cross-domain attention for structural localization) contributes +4.9% vitiligo and +1.7% DRIVE. Notably, module combinations exhibit synergistic effects: **STFF+SFI** performs exceptionally well (+4.8% DRIVE over baseline), reflecting complementary global frequency alignment and local attention. The full AFDAN (all modules integrated) achieves the highest IoU: 90.9% (+10.6% vitiligo) and 82.6% (+6.1% DRIVE), validating the modules’ collaborative enhancement of cross-domain adaptation under annotation scarcity.

## 4. CONCLUSION

In this paper, we have proposed AFDAN, a novel cross-domain segmentation network designed to tackle annotation scarcity in medical imaging. The framework integrates three core modules: an Adversarial Domain Learning module that aligns feature distributions via frequency transformation, a Source–Target Frequency Fusion module that accelerates adaptive feature construction, and a Spatial-Frequency Integration module that combines complementary representations to preserve structural details. Extensive experiments show that AFDAN achieves state-of-the-art performance, with a 90.9% IoU on VITILIGO2025 and 82.6% IoU on the DRIVE benchmark. The results confirm its robustness in segmenting both normal and pathological regions with high fidelity, demonstrating strong potential for clinical applications where annotated data are limited.

## 5. REFERENCES

- [1] J. Cheng, B. Fu, J. Ye, G. Wang, T. Li, H. Wang, R. Li, H. Yao, J. Cheng, J. Li, Y. Su, M. Zhu, and J. He, "Interactive medical image segmentation: A benchmark dataset and baseline," in *CVPR*, 2025.
- [2] Y. Ganin, E. Ustinova, H. Ajakan, P. Germain, H. Larochelle, F. Laviolette, M. Marchand, and V. Lempitsky, "Domain-adversarial training of neural networks," *Journal of Machine Learning Research*, vol. 17, no. 1, pp. 1–35, 2016.
- [3] S. Kyung Jeon, I. Joo, J. Park, J. Kim, S.J. Park, and S.H. Yoon, "Fully-automated multi-organ segmentation tool applicable to both non-contrast and post-contrast abdominal CT: deep learning algorithm developed using dual-energy CT images," *Scientific Reports*, vol. 14, no. 1, pp. 4378, 2024.
- [4] Y. Yang and S. Soatto, "FDA: Fourier domain adaptation for semantic segmentation," in *CVPR*, 2020.
- [5] S. Asutkar and S. Tallur, "Deep transfer learning strategy for efficient domain generalisation in machine fault diagnosis," *Scientific Reports*, vol. 13, 2023.
- [6] Y. Fu, M. Zhang, X. Xu, Z. Cao, C. Ma, Y. Ji, K. Zuo, and H. Lu, "Partial feature selection and alignment for multi-source domain adaptation," in *CVPR*, 2021, pp. 16654–16663.
- [7] H. Yang, N. Wang, Z. Wang, L. Wang, and H. Li, "Consistency-guided pseudo labeling for transductive zero-shot learning," *Information Sciences*, vol. 670, pp. 120572, 2024.
- [8] S. Chen, X. Zhao, M. Liu, and J. Zhou, "Frequency-domain domain generalization for skin lesion segmentation with scarce annotations," *Medical Image Analysis*, vol. 85, pp. 102789, 2023.
- [9] Q. Pan, Y. Xue, and B. Yang, "A deformable-based source-free unsupervised domain adaptation method for cervical cell detection," in *ICASSP*, 2025.
- [10] J. Huang, D. Guan, A. Xiao, and S. Lu, "Fsdr: Frequency space domain randomization for domain generalization," in *CVPR*, 2021, pp. 6891–6902.
- [11] L. Guo, Y. Yang, H. Ding, H. Zheng, H. Yang, J. Xie, Y. Li, T. Lin, and Y. Ge, "A deep learning-based hybrid artificial intelligence model for the detection and severity assessment of vitiligo lesions," *Annals of Translational Medicine*, vol. 10, no. 10, pp. 590, May 2022.
- [12] J. Staal, M.D. Abramoff, M. Niemeijer, M.A. Viergever, and B. van Ginneken, "Ridge-based vessel segmentation in color images of the retina," *IEEE Transactions on Medical Imaging*, vol. 23, no. 4, pp. 501–509, 2004.
- [13] P. Chattopadhyay, K. Sarangmath, V. Vijaykumar, and J. Hoffman, "PASTA: Proportional amplitude spectrum training augmentation for syn-to-real domain generalization," in *ICCV*, 2023.
- [14] I. Lee, W. Lee, and H. Myung, "Domain generalization with vital phase augmentation," in *Proc. of the AAAI Conference on Artificial Intelligence*, 2024.
- [15] K. Zhang and X. Zhuang, "Cyclemix: A holistic strategy for medical image segmentation from scribble supervision," in *CVPR*, 2022.
- [16] L. Luo, B. Xu, Q. Zhang, C. Lian, and J. Luo, "A fourier transform framework for domain adaptation," in *Chinese Conference on Pattern Recognition and Computer Vision (PRCV)*. Springer, 2024, pp. 19–33.
- [17] X. Jiang, Z. Zhou, H. Wang, G. Wang, and Z. Fang, "Texliver-net: Leveraging medical knowledge and spatial-frequency perception for enhanced liver tumor segmentation," in *IEEE International Symposium on Biomedical Imaging (ISBI)*, 2025.
- [18] V. VS, V. Gupta, P. Oza, V. A. Sindagi, and V. M. Patel, "MeGA-CDA: Memory guided attention for category-aware unsupervised domain adaptive object detection," in *CVPR*, 2021.
- [19] E. Xie, W. Wang, Z. Yu, A. Anandkumar, J. M. Alvarez, and P. Luo, "SegFormer: Simple and efficient design for semantic segmentation with transformers," *Advances in neural information processing systems*, vol. 34, pp. 12077–12090, 2021.
- [20] N. C. F. Codella, D. Gutman, M. E. Celebi, B. Helba, M. A. Marchetti, S. W. Dusza, A. Kalloo, K. Liopyris, N. Mishra, H. Kittler, and A. Halpern, "Skin lesion analysis toward melanoma detection: A challenge at the 2017 international symposium on biomedical imaging (isbi), hosted by the international skin imaging collaboration (isic)," in *IEEE International Symposium on Biomedical Imaging (ISBI)*, 2018.
- [21] W. Yuan, J. Wang, and W. Xu, "Shift pooling PSPNet: Rethinking PSPNet for building extraction in remote sensing images from entire local feature pooling," *Remote Sensing*, vol. 14, no. 19, 2022.
- [22] N. Ravi, V. Gabeur, Y.-T. Hu, R. Hu, C. Ryali, T. Ma, H. Khedr, R. Rädle, C. Rolland, L. Gustafson, and et al., "SAM 2: Segment anything in images and videos," *arXiv preprint arXiv:2408.00714*, 2024.
- [23] Y. Zhu, C. Shi, D. Wang, J. Tang, Z. Wei, Y. Wu, G. Li, and S. Yang, "Rethinking query-based transformer for continual image segmentation," in *CVPR*, June 2025.
- [24] Q. Bi, S. You, and T. Gevers, "Learning content-enhanced mask transformer for domain generalized urban-scene segmentation," in *Proceedings of the AAAI Conference on Artificial Intelligence*, 2024.
- [25] Ultralytics, "YOLO 11: State-of-the-art real-time object detection," Computer software, available at <https://github.com/ultralytics/ultralytics>, 2024, Accessed on September 6, 2024.
- [26] J. Li, Z. Wang, Y. Gao, and X. Hu, "Exploring high-quality target domain information for unsupervised domain adaptive semantic segmentation," in *Proceedings of the 30th ACM International Conference on Multimedia*, 2022, pp. 5237–5245.
- [27] Y. Gao, Z. Wang, and Y. Zhang, "Delve into source and target collaboration in semi-supervised domain adaptation for semantic segmentation," in *ICME. IEEE*, 2024, pp. 1–6.
- [28] Z. Deng, W. Gao, Z. Gong, R. Gan, L. Chen, S. Zhang, and L. Ma, "A fundus image dataset for ai-based artery-vein vessel segmentation," *Scientific Data*, vol. 12, no. 1, pp. 1298, 2025.